Korean Journal of Remote Sensing, Vol.36, No.1, 2020, pp.1~13
https://doi.org/10.7780/kjrs.2020.36.1.1

ISSN 1225-6161 (Print)
ISSN 2287-9307 (Online)

Article

Seasonal Water Change Assessment at Mahanadi River, India using Multi-temporal Data in Google Earth Engine

Ratiranjan Jena[1] · Biswajeet Pradhan [2]† · Hyung-Sup Jung [3] · Abhishek Kumar Rai [4] · Hossein Mojaddadi Rizeei [5]

Abstract : Seasonal changes in river water vary seasonally as well as locationally, and the assessment is essential. In this study, we used the recent technique of post-classification by using the Google earth engine (GEE) to map the seasonal changes in Mahanadi river of Odisha. However, some fixed problems results during the rainy season that affects the livelihood system of Cuttack such as flooding, drowning of children and waste material deposit. Therefore, this study conducted 1) to map and analyse the water density changes and 2) to analyse the seasonal variation of river water to resolve and prevent problem shortcomings. Our results showed that nine types of variation can be found in the Mahanadi River each year. The increase and decrease of intensity of surface water analysed, and it varies in between -130 to 70 m^3/nf. The highest frequency change is 2900 Hz near Cuttack city. The pi diagram provides the percentage of seasonal variation that can be observed as permanent water (30%), new seasonal (28%), ephemeral (12%), permanent to seasonal (7%) and seasonal (10%). The analysis is helpful and effective to assess the seasonal variation that can provide a platform for the development of Cuttack city that lies in Mahanadi delta.

Key Words : Mahanadi River, Remote sensing, GIS, Seasonal Variation, Water density

1. Introduction

Assessment of the mapping of seasonal variation of river water is essential that can be evaluated through different aspects of seasonal changes analysis. Ground water and surface water changes mainly depend on

Received August 10, 2019; Revised August 20, 2019; Accepted September 6, 2019; Published online October 1, 2019

[1] PhD Student, The Centre for Advanced Modelling and Geospatial Information Systems (CAMGIS), University of Technology Sydney
[2] Distinguished Professor, The Centre for Advanced Modelling and Geospatial Information Systems (CAMGIS), University of Technology Sydney
[3] Professor, Department of Geoinformatics, University of Seoul
[4] Assistant Professor, Centre for Oceans, Rivers, Atmosphere and Land Sciences (CORAL), Indian Institute of Technology Kharagpur
[5] Postdoctoral Research Associate, The Centre for Advanced Modelling and Geospatial Information Systems (CAMGIS), University of Technology Sydney

† Corresponding Author: Biswajeet Pradhan (biswajeet.pradhan@uts.edu.au)

This is an Open-Access article distributed under the terms of the Creative Commons Attribution Non-Commercial License (http://creativecommons.org/licenses/by-nc/3.0) which permits unrestricted non-commercial use, distribution, and reproduction in any medium, provided the original work is properly cited.

some input sources of natural and anthropogenic points. The features that can be found in the surface water are distinctly direct toward different seasons. Monitoring and detection of various changes by applying different applications of remote sensing have been widening the research all over the world (Rokni *et al*., 2014). Many researchers and scientists have proposed several remote sensing applications such as; land changes monitoring and mapping, vegetation change monitoring, disaster forecasting, urban sprawl applications and hydrological modelling (Bagan *et al*., 2012; Jena *et al*., 2019; Al-shalabi *et al*., 2013). However, the river is precisely a unique resource for human survival. Therefore, it is an essential part of human life that helps in developing a balanced ecosystem. The spatial distribution of river water provides several reliable information, which is important for real-world applications, such as the assessment of future water resources, climatic modelling, suitability for agriculture, dynamics of a river system, wetland inventory, watershed management, surveying river catchment, flood modelling, and many other monitoring applications (Alley *et al*., 1999; Rokni *et al*., 2014; Salmon *et al*., 2013; Demir *et al*., 2013; Volpi *et al*., 2013; Hong *et al*., 2016). A significant amount of remote sensing data source is freely available for landuse/ landcover extraction (Ridd and Liu, 1998). Seasonal variation of river water mostly depends on natural geomorphological processes such as precipitation, weathering, erosion, as well as some anthropogenic impacts on urban and industrial activities (Brisco *et al*., 2013). River water gets contaminated easily due to its exposure to various pollutants (Lu *et al*., 2011). However, the river discharge and subsequent variation by extreme changes in frequency in rivers are generally influenced by seasonal variations that depend on the hydrologic processes within the basin (Rokni *et al*., 2014).

Different image processing techniques have been used by many researchers in the current period for the water feature extraction and seasonal variation mapping from different types of satellite data (Xu *et al*., 2010; Aziz *et al*., 2019). Single-band methods are mostly used for the feature extraction (Kaliraj *et al*., 2012). Classification techniques applied for the seasonal changes analysis that provides better accuracy as compared to single-band methods (Raja *et al*., 2013). Multi-band approach used different reflective bands for improvement of change detection (Markogianni *et al*., 2013). For instance, the Normalized Difference Water Index (NDWI) has been applied by scientists using Landsat imagery (Bagan, 2012). The Modified Normalised Difference Water Index (MNDWI) only extracts changes in river water by suppressing vegetation, soil and builtup areas (Lu *et al*., 2011). River water seasonal variation is usually conducted by individual feature extraction from the multi-date satellite images (Pradhan *et al*., 2014).

In this study, the seasonal variation of river Mahanadi in Cuttack, Odisha during 2012-2017 was investigated. Mahanadi River, with an area varying from 141,600 km^2 during the recent century is the largest river in Odisha (Panda *et al*., 2006). Changes in surface water can be found specifically in summer and driven by water managers. The river water intensity changes after 2012 were analysed and the change of intensity was calculated. Out of several Indian seasonal rivers, Mahanadi River is the river connected with many mountainous streams; however, it is difficult to pinpoint the exact source. The headwaters of Mahanadi River lie at 6 Kms from village Pharsiya about 442 m (1,450 ft.) above mean sea level (MSL) in Chhattisgarh district (Upadhyay, 1998). The hills in this area are an extension of the Eastern Ghats and are a source of many other streams, which then join the Mahanadi. The delta structure developed in the Cuttack and Puri district in Odisha supplying a high amount of sediments into the Bay of Bengal (Upadhyay, 1998). The ancient city Cuttack is established in that delta, helping in the Odisha's economic development. Seasonal floods are common every year. To tackle these problems, some research needs to analyse the seasonal changes of the river as well as the intensity of water at a particular period. Therefore, we have used remote sensing to address this issue.

The major problems that affect the city population, transportation and environment is flooding. The Cuttack city lies on a river locked land of Mahanadi delta. The size of the delta increases every year because of a huge amount of sediment deposit by the river. However, the irrigation system of the city is not well designed. Therefore, flooding during rainy season creates multitude problems. The main aim of the current study is to establish an effective methodological approach by using GEE for the mapping of seasonal variation in surface water of Mahanadi river basin, Odisha. Several surface water extraction techniques were applied in different rivers and lakes appropriately as well as the suitable techniques have been already applied to detect and map the spatio-temporal variation in different locations. However, there is no effective analysis conducted till date on Mahanadi River in Cuttack delta to map the seasonal variation. Subsequently, we have applied a compelling and well-developed approach using GEE for seasonal variation mapping and to measure change in water intensity.

2. Data and Methodology

1) Study area

The Mahanadi is one of the major rivers in the East and Central parts of India (Fig. 1). The drained area of the river is 141,600 km^2 approximately (54,700 Mi^2) and 858 km of total course. The river is wide near the Cuttack city, developing into a delta structure. The Mahanadi is widely famous for the Hirakud Dam that

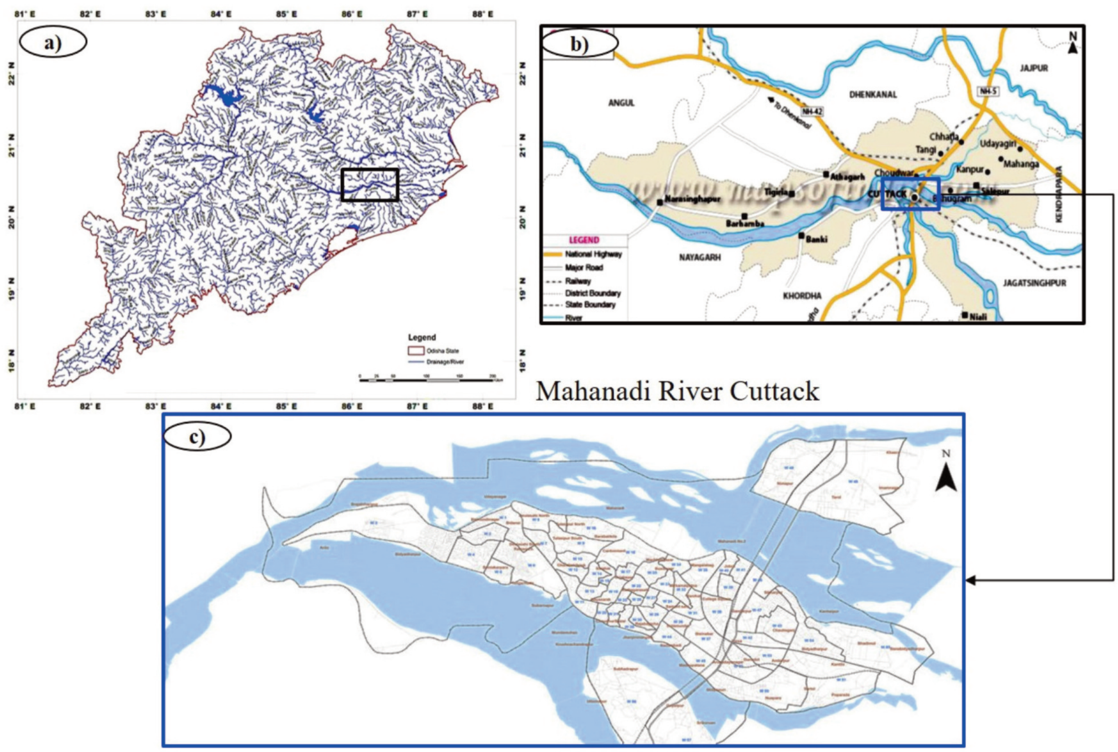

Fig. 1. Study area.

Source: Published in Maps of India map site (Sandrp, 2016).

Table 1. Environmental condition that will affect the seasonal variability of Mahanadi River in Cuttack

	Pre-monsoon	Post-monsoon	Summer	Total
Catchment area (Sq. km)				141,134
Annual flow (Mm^3)				51,061
Drainage area (Sq. km)				65,579
Annual rainfall (mm)				1334.5
Sediments				Delta deposit and unconsolidated quaternary formation (Sandstone, sand, clay) Precambrian basement
Temperature (Degree Celsius)	30	28	28	
PH	8.2	7.9	8.3	
Salinity (ppt)	9.6	10.9	27	
Ground water variation in Cuttack city (mbgl)	0.66	–	10.5	

Source: Central Groundwater Information Booklet published by Central Groundwater Board of India (CGWI).

connects a large area of irrigation. The river flows and connects the states of Chhattisgarh, Odisha, Maharashtra and Bihar. Mahanadi River delta deposits a large amount to the Bay of Bengal as the river basin drains a high amount of sediments. The meandering of the Mahanadi River can be found in Chhattisgarh and in some part of Odisha that changes its course. The length of the Mahanadi River is around 900 Kms. Silt is more in Mahanadi than any other sediments in the Indian subcontinent. The drainage basin covers an area of approximately 141,464 km^2 (Sundaray *et al*., 2011). The study area of Mahanadi River is the part surrounding the Cuttack city lies at lat. and long. of 20°31’25″N and 85°47’17″E, respectively. The Cuttack city in the delta is very popular and well known for the famous stadium and large city infrastructure. The city ranked 72 in India as a populated city. The total population in the city is around 606,007 (Sundaray *et al*., 2011). The City area is water locked by Mahanadi and Kathajodi River as described previously (Sandrp, 2016). The detailed description of the seasonal environmental condition of Mahanadi River is presented in Table 1.

2) Data

The technical descriptions about the data that was used in this research are assessable in the GEE. The availability of data is an open source and can be downloaded from the data access section of the USGS (US Geological Survey) website. The website also provides some ancillary files that can help during data processing, such as metadata files and symbologies. This analysis was conducted using the open source Landsat 7 data. The data that can be found in the GEE workspace or from the USGS earth explorer with multi-band assets. The 2012 and 2017 used to analyse in this research. The datasets that are used here are intended to show different facets of the spatial and temporal distribution of surface water over the last five years. Therefore, the datasets can be used to map the seasonality variation, and some datasets intended to project the temporal change in specific areas.

3) Methodology

To achieve the aim in this work, some process was performed as presented in Fig. 2. Identifying the study area that defines the problems, finding the open access data sources, image processing, careful analysis, observation for river water change intensity mapping and seasonal variation monitoring using effective modelling approach.

To prepare the input Landsat image in GEE, the coding for the pre-processing of the data needed (Ghasemi *et al*., 2018). Different pre-processing steps can be performed using the GEE, such as radiometric calibration, atmospheric correction (Gorelick *et al*., 2017; Pradhan *et al*., 2018). Radiometric calibration and atmospheric correction need to be conducted to find accurate results. For doing this, the images were converted to at-satellite radiance using the tool Landsat calibration in ENVI 5.3. Afterwards, the required information from the data can be clearly seen in the GEE. The GEE is used to make the personal account, edit and write the code. The processing of the data can be started from the uploading of the data in the GEE workspace. The outlook of the loaded data can be understood clearly from the loaded screen of GEE. Surface water extraction and intensity measurement by mask using Landsat 8 imagery was challenging. There is a requirement of a newly developed approach to derive the water mask from different types of imagery. The method behind the GEE considers the use of the MNDWI Spectral Index (Equation 2). However, it is an interesting approach with a non-parametric detection of local thresholds to improve detection accuracy. The MNDWI is approximately similar to the NDWI Spectral Index (Equation 1) that uses a shortwave infrared band without using the near-infrared. Additional steps of the Normalized Difference Vegetation Index (NDVI) needed (Equation 3) to remove the false water detection in a heavily vegetated area by using a high threshold value of 0.3.

$$NDWI = (\rho green - \rho nir) / (\rho green + \rho nir) \quad (1)$$

$$MNDWI = (\rho green - \rho swir) / (\rho green + \rho swir) \quad (2)$$

$$NDVI = (\rho nir - \rho red) / (\rho nir + \rho red) \quad (3)$$

Where, ρgreen, ρswir1, ρnir, and ρred represent TOA reflectance for corresponding Landsat 7 bands.

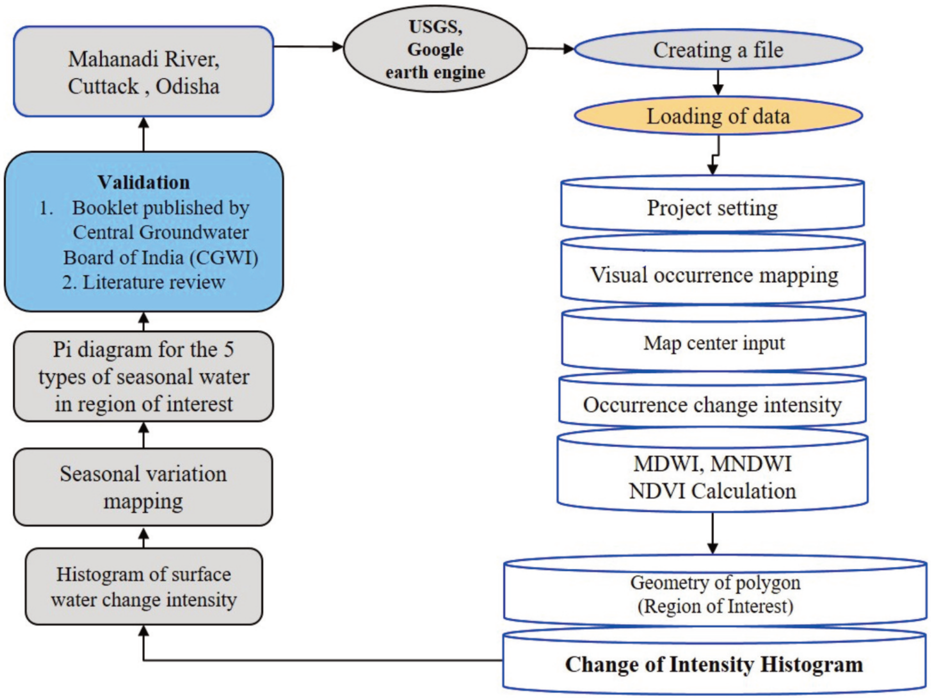

Fig. 2. Shows the overall methodology to map the river water seasonal variation.

In the first step, the data should be analysed to determine the water occurrence in a particular period of 2012. For the visual occurrence of water in the river, the palette used here is red and blue. The values are assigned to the visual occurrence can be found between 0 and 100. In the next step, visual changes of the river water need to be analysed. The palette used here is generally red, black, and lime green with a minimum values of -50 and a maximum of 50. In the next step, the region of interest is chosen for seasonality analysis. However, the region is classified into different transition classes. In total, nine transition classes of seasonal variation can be found in the region of interest considered as the significant changes. Nevertheless, in total five major types of classes can be observed in the study area. Eventually, the frequency of water intensity changes and the percentage of transition class areas are presented in the graph.

3. Results and Discussions

The frequency of surface water occurrence (SWO) was analysed in this study from 2012 to 2017. The water detections (WD) along with valid observations (VO) are summed to compute the SWO values (Tang *et al*., 2013). Averaging the results of SWO calculations that provide the values of surface water occurrence. The water occurrence needs to be understood for the next step of seasonal variation analysis. Change of occurrence of surface water intensity between the periods 2012 to 2017 was mapped and analysed.

Fig. 3 classifies the study area into four different classes, such as; water body, vegetation, sand and lithology. Then the water occurrence analysis conducted. This can be derived from a homologous pair's analysis of months. The occurrence difference between periods was computed for each pair and differences between all homologous pairs of months were then averaged to create the surface water occurrence change intensity map. Areas, where there are no pairs of homologous months, could not be mapped. Averaging of the monthly processing mitigates variations in data distribution over time (that is, both seasonal variation in the distribution of valid observations, temporal depth and frequency of observations through the archive) and provides a consistent estimation of the water occurrence change. Water occurrence change dataset was analysed and presented in Fig. 4.

The details of the permanent water area mapped by using the water mask analysis. However, the permanent water area and non-water areas were identified in

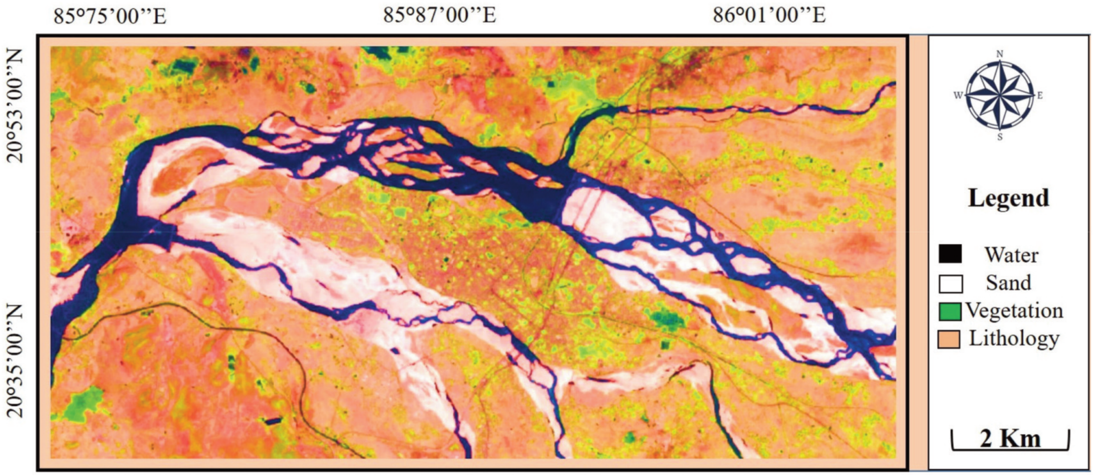

Fig. 3. Classification of the study area.

Fig. 5. Increase in water intensity is presented in green, and decreased intensity is presented in red colour. There is no significant change can be found in black areas in the water that occurs during the period 2012 -2017. The projected colour represents the degree of change occurring in the surface water. Bright red areas represent a greater loss of surface water than light red areas. Grey colour areas appear on the map and are the locations with insufficient data to compute the change statistics.

The intensity changes are mapped and projected in Fig. 6. The map is divided into four classes with 100% water, 1% water, no water and no data, respectively in the water occurrence map while the water intensity change map indicates the different classes of a 100% increase of water intensity, 100% loss, no change and no data.

A permanent water body can be defined as it stays throughout the year when a seasonal water body stays for less than 12 months in a year. We focus our observation for all the locations surrounding the Cuttack city. River water is considered seasonal if the number of months, where water present is less than the months where valid observations were acquired. Another point that needs to take into consideration is the freezing of some parts of the river or lakes for some

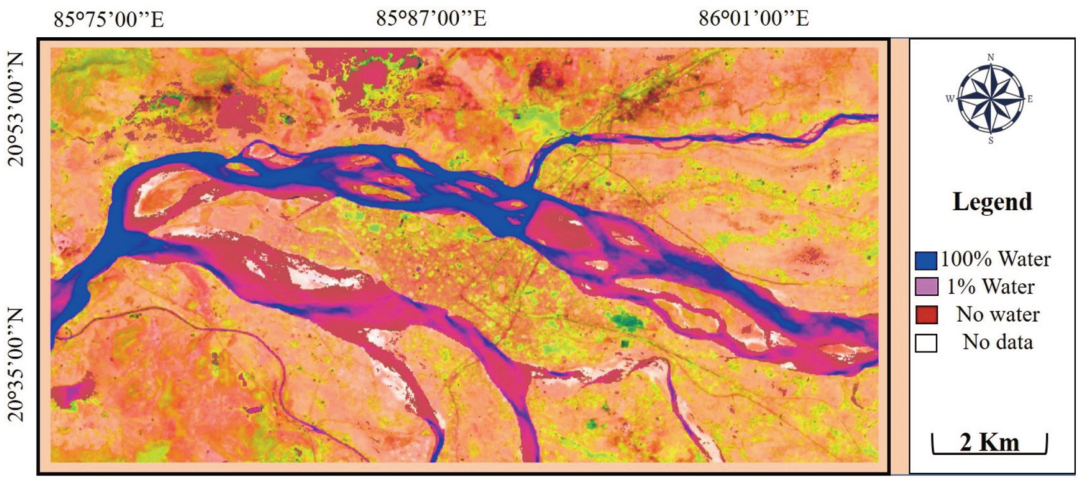

Fig. 4. Water occurrence during 2012.

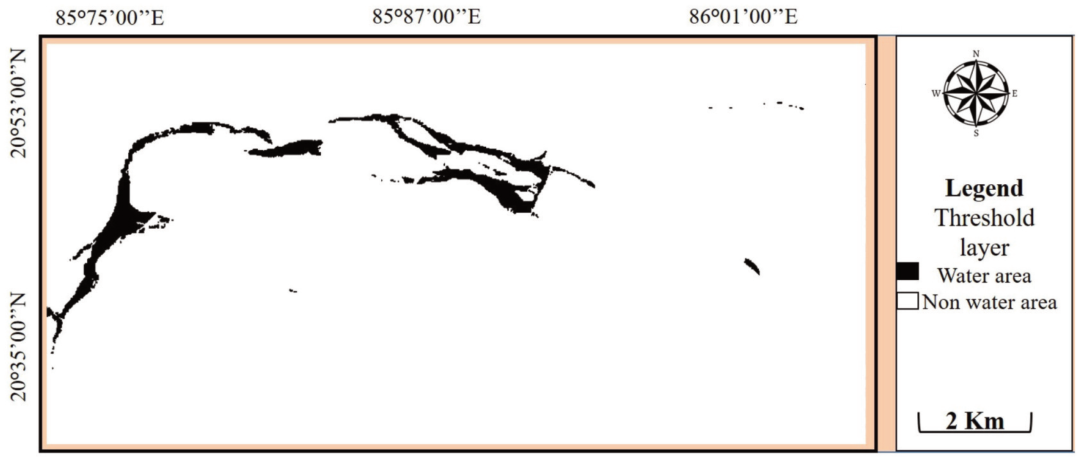

Fig. 5. Permanent water area by masking.

part of a year (Dronova *et al*., 2011). Nevertheless, water is still present in the ice layer. In general, during the application of the method, ice should be treated as a non-valid observation. However, we did not face any problem like ice in the Mahanadi River, as it is present in a tropical region. Throughout the observation period, if the water is present at a constant level can be called a permanent water surface. If any changes can be found during the observation period that can be represented as a seasonal water surface. Seasonality can be computed for each year.

Generally, the thematic maps are used for the water class identification that can be separated by a transition zone between the first and last year observations. The recurrence water class and the temporal profiles need to be analysed for the representative years. This analysis observes the classified water in a particular given month and continuously added one by one for the whole year. If a year contains a sufficient amount of effective and valid observations from a combining approach of months with confidence for the presence or absence of water determination, then it can be flagged as representative. The confidence can be determined by the sum of the monthly-observed recurrences. However, the lack of water can be described by the seasonal shift that may not provide a level of confidence to conclude that the water was not available there. Therefore, what we considered in this analysis is that if the sum of recurrence of months is crossover 100, the water absence provides a high level of confidence to observe that there was no water. Conversely, a single water presence is sufficient to explain the presence of water. The first water class is regarded as the first year while the last year's water class is the last class, which is assigned just because of the last year of observation. However, there are several observations available within a year in a particular period.

The different transition classes were observed and mapped, such as; permanent water areas; new permanent water areas (conversion of a land into permanent water); new seasonal water surfaces (conversion of land part into seasonal water); conversion of permanent water into seasonal water; unchanging seasonal water surfaces; lost seasonal water surfaces (conversion of seasonal water into land); and the conversion of seasonal water into permanent water; lost permanent water areas (conversion of permanent water into land part);. In total, 5 major types of seasonal variation were seen in the region of interest characterised by permanent (30%), new seasonal (28%), ephemeral (12%), permanent to seasonal (7%) and seasonal (10%). The region of interest was applied to the river

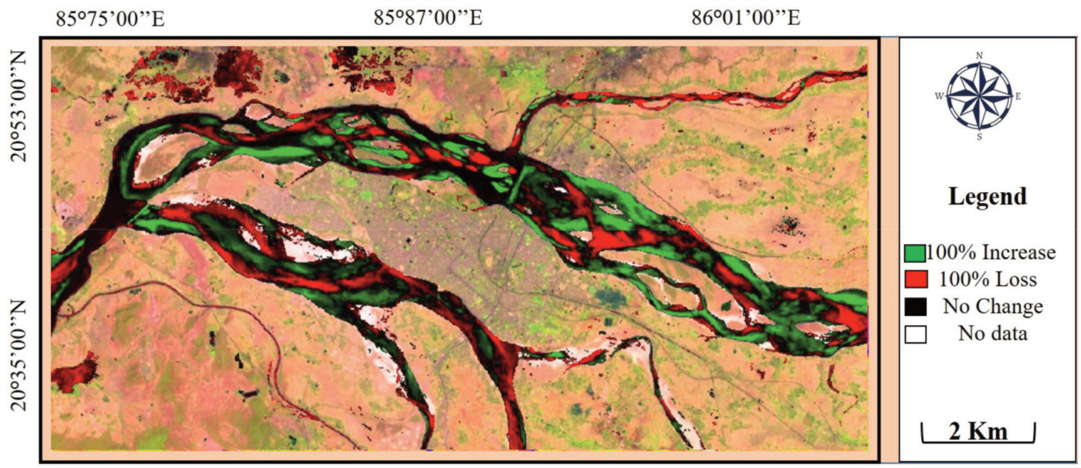

Fig. 6. Water intensity change during 2017.

area only surrounding the Cuttack city can be seen in Fig. 7. Therefore, the percentage of transition classes only analysed and presented through the pi-diagram. The transition classes are mapped and presented in Fig. 7(b). It was classified into nine classes, however, there are five major transition classes (permanent, new seasonal, ephemeral, permanent to seasonal and seasonal) can be seen in the study area, affecting the Cuttack city.

Fig. 8 and 9 represent the water intensity change and the percentage of seasonal variation that occurred in the different parts of the river within the region of interest, respectively. Histogram of water intensity variation indicates that the intensity increases and decreases spatially along with the change in frequency. The highest frequency was 2900 Hz with a change of intensity of 10 m^3/nf. The intensity of Mahanadi River water varies from -130 to 70 m^3/nf. The intensity value provides an exclusive message of water level rise and fall that can affect the groundwater flow system. The conversions are called as changes that can be found from the starting and finishing points of the time series. An unchanging permanent water area explains that the seasonality at a specific area was the same in starting and in the ending year of analysis without a stability necessity. Stability should be analysed at the pixel scale by considering the long-term history of river water that is described by the temporal profiles along with the

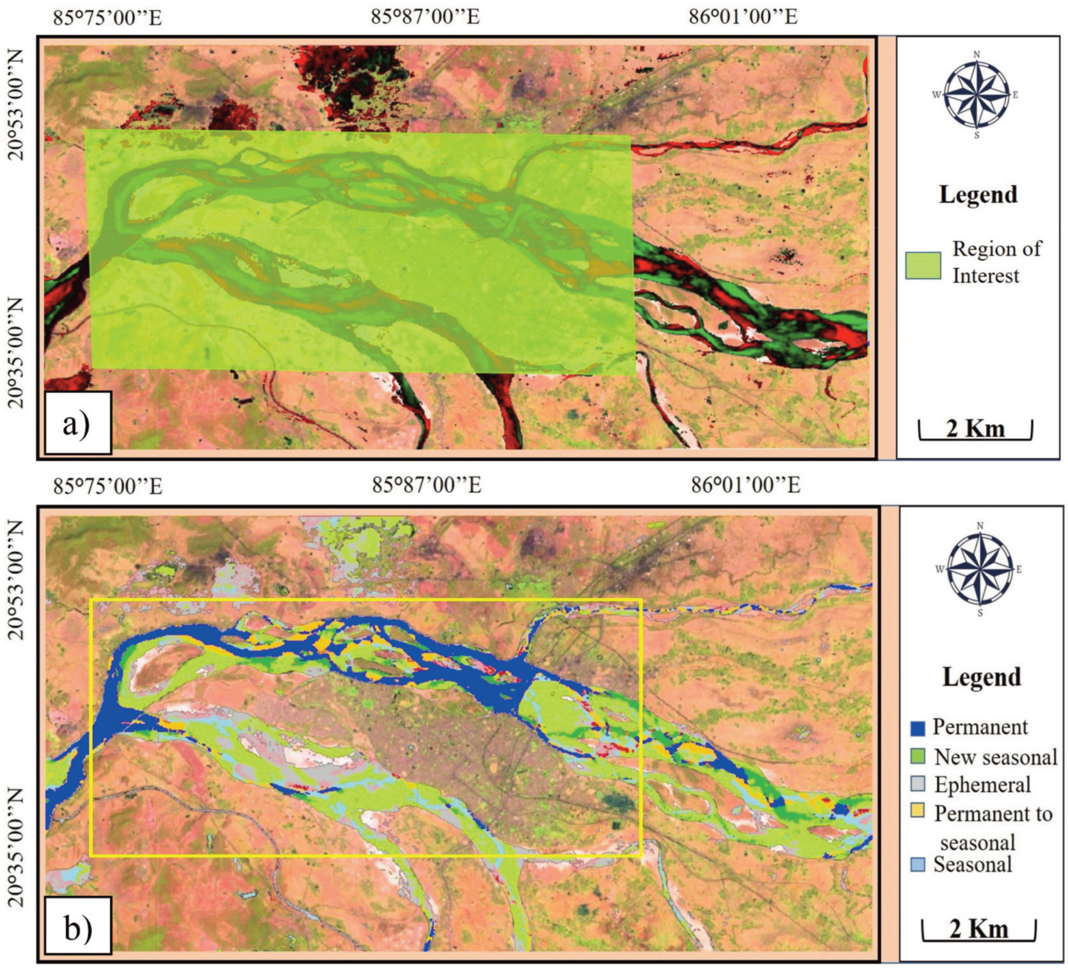

Fig. 7. a) Region of interest for the seasonal variation mapping; b) Seasonal variation mapped areas.

occurrence and recurrence maps. Some instances can be possible, where no water at the beginning or the end but observed in some intervening years.

By analysing the inter-annual patterns and their intra-annual event characteristics, each pixel should be provided with a different class value for ephemeral permanent water (land replaced by permanent water that subsequently disappears) or ephemeral seasonal water (land replaced by seasonal water that subsequently disappears) that depends on the period of water presence and a majority of seasonality. However, in every year the surface water variation occurs that depends on various factors as well as human activities. Seasonal variation and intensity change detection are significant that can provide valuable climatic information in that area. Therefore, for the development of the city environment and future research analysis, implementation of a new technique is important.

4. Conclusions

Transition classes are generally influenced by various meteorological and hydrological phenomena. The effects of all these factors, specifically wind speed, freshwater diversions, and river discharge, control the

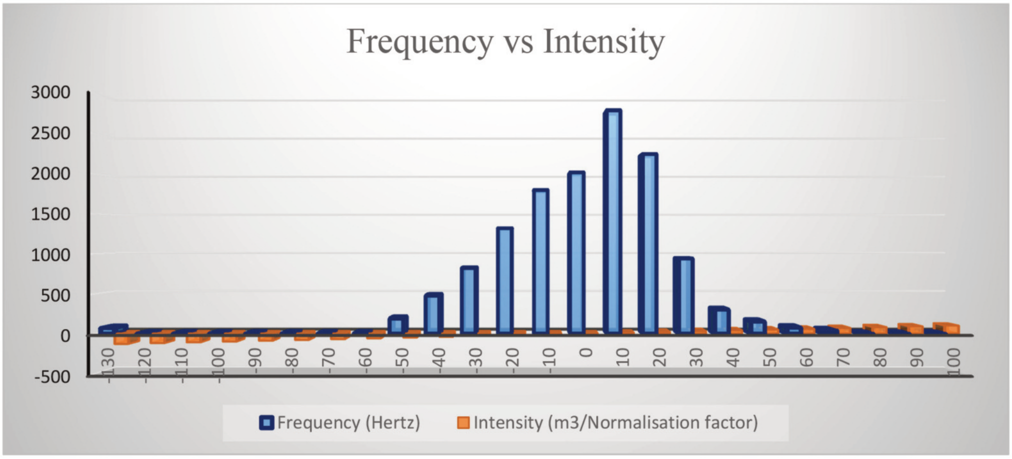

Fig. 8. Histogram of water intensity variation.

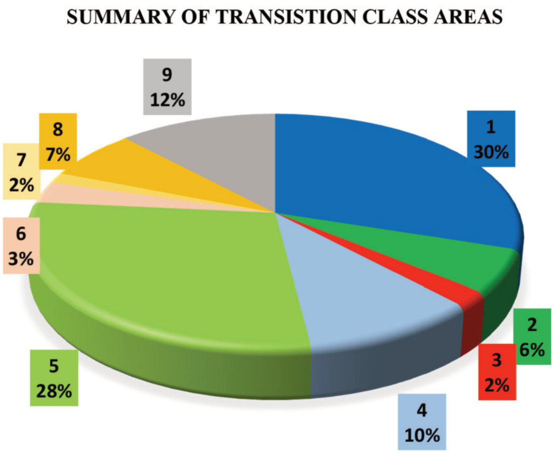

Value	Label
1	Permanent
2	New permanent
3	Lost permanent
4	Seasonal
5	New seasonal
6	Lost seasonal
7	Seasonal to permanent
8	Permanent to seasonal
9	Ephemeral permanent

Fig. 9. Percentage of transition classes.

spatial and seasonal variability in the Mahanadi River. Our output shows that five main transition classes can be found in this region. Many factors that create a strong influence in result such as; meteorological seasonally dependent factors, limited temporal and spatial resolution of the data, and the optical interference of particulate matter, skylight and whitecaps on the water leaving radiance. Although the proposed methodology has been applied to some other study areas, and it works well in Mahanadi River, it could be subject to change in the resolution, coefficients of a regression function if needed to apply in any other river. Nonetheless, the performance of the methodology using GEE supports the quality of Landsat data for this effective research. A necessary step needs to consider for the effective result in GEE if it considers a complete package of the hydrological and meteorological factors in the development of a novel algorithm. The results obtained from this research can be used in developing a strategy for water protection measures. This can be used as a base for the prevention of extreme pollution, designing of treatment strategy and in improving the standard water quality, determination of not only concentrations of ingredients but also the excess probabilities value in the water. Concluding, the seasonal variation of surface water depends on various factors. Therefore, all the hydrological and meteorological factors need to be considered for the betterment of results in a future study on the Mahanadi River.

Acknowledgements

Authors are thankful to the University of Technology Sydney for the technical support and for providing the remote sensing software. This research is funded by the Centre for Advanced Modelling and Geospatial Information Systems (CAMGIS), UTS grant numbers 321740.2232335, 323930, and 321740.2232357; 321740.2232424; and 321740.2232452. And this research was also supported by the National Research Foundation of Korea (NRF) grant funded by the Korea government (MSIT) (No. 2019R1F1A1059570). In addition, this research was supported by a grant (18SIUE-B148326-01) from Satellite Information Utilization Center Establishment Program by Ministry of Land, Infrastructure and Transport of Korean government.

References

Alley, W.M., T.E. Reilly, and O.L. Franke, 1999. *Sustainability of Groundwater Resources*, U. S. Geological Survey (U.S.GS), Denver, CO, USA.

Al-shalabi, M., L. Billa, B. Pradhan, S. Mansor, and A.A. Al-Sharif, 2013. Modelling urban growth evolution and land-use changes using GIS based cellular automata and SLEUTH models: the case of Sana'a metropolitan city, Yemen, *Environmental Earth Sciences*, 70(1): 425-437.

Azeez, O.S., B. Pradhan, R. Jena, H.S. Jung, and A.A. Ahmed, 2019. Traffic Emission Modelling Using LiDAR Derived Parameters and Integrated Geospatial Model, *Korean Journal of Remote Sensing*, 35(1): 137-149.

Bagan, H. and Y. Yamagata, 2012. Landsat analysis of urban growth: How Tokyo became the world's largest megacity during the last 40 years, *Remote Sensing of Environment*, 127: 210-222.

Brisco, B., A. Schmitt, K. Murnaghan, S. Kaya, and A. Roth, 2013. SAR polarimetric change detection for flooded vegetation, *International Journal of Digital Earth*, 6(2): 103-114.

Demir, B., F. Bovolo, and L. Bruzzone, 2013. Updating land-cover maps by classification of image time series: A novel change-detection-driven transfer learning approach, *IEEE Transactions on Geoscience and Remote Sensing*, 51(1):

300-312.

Dronova, I., P. Gong, and L. Wang, 2011. Object-based analysis and change detection of major wetland cover types and their classification uncertainty during the low water period at Poyang Lake, China, *Remote Sensing of Environment*, 115 (12): 3220-3236.

Ghasemi, K., B. Pradhan, and R. Jena, 2018. Spatial Identification of Key Alteration Minerals Using ASTER and Landsat 8 Data in a Heavily Vegetated Tropical Area, *Journal of the Indian Society of Remote Sensing*, 46(7): 1061-1073.

Government of India central ground water board, Ministry of Water Resources & Ganga Rejuvenation, South Eastern Region Bhubaneswar, 2017. Ground water year book 2016-2017, http://cgwb.gov.in/Regions/GW-year-Books/GWYB-%202016-17/Orissa.pdf, Accessed on Feb. 15, 2019.

Google Earth Engine, 2012. https://earthengine.google.com, Accessed on Feb. 5, 2017.

Gorelick, N., M. Hancher, M. Dixon, S. Ilyushchenko, D. Thau, and R. Moore, 2017. Google Earth Engine: Planetary-scale geospatial analysis for everyone, *Remote Sensing of Environment*, 202: 18-27.

Hong, H., S.A. Naghibi, H.R. Pourghasemi, and B. Pradhan, 2016. GIS-based landslide spatial modelling in Ganzhou City, China, *Arabian Journal of Geosciences*, 9(2): 112.

Jena, R., B. Pradhan, G. Beydoun, H. Sofyan, and M. Affan, 2019. Integrated model for earthquake risk assessment using neural network and analytic hierarchy process: Aceh province, Indonesia, *Geoscience Frontiers*, https://doi.org/10.1016/j.gsf.2019.07.006.

Kaliraj, S., S. Muthu Meenakshi, and V.K. Malar, 2012. Application of remote sensing in detection of forest cover changes using geo-statistical change detection matrices- A case study of devanampattu reserve forest, tamilnadu, India, *Nature Environment and Pollution Technology*, 11(2): 261-269.

Lu, S., B. Wu, N. Yan, and H. Wang, 2011. Water body mapping method with HJ-1A/B satellite imagery, *International Journal of Applied Earth Observation*, 13(3): 428-434.

Markogianni, V., E. Dimitriou, and D.P. Kalivas, 2013. Land-use and vegetation change detection in plastira artificial lake catchment (Greece) by using remote sensing and GIS techniques, *International Journal of Remote Sensing*, 34(4): 1265-1281.

Panda, U.C., S.K. Sundaray, P. Rath, B.B. Nayak, and D. Bhatta, 2006. Application of factor and cluster analysis for characterization of river and estuarine water systems–a case study: Mahanadi River (India), *Journal of Hydrology*, 331(3-4): 434-445.

Pradhan, B., A.A.A. Moneir, and R. Jena, 2018. Sand dune risk assessment in Sabha region, Libya using Landsat 8, MODIS, and Google Earth Engine images, Geomatics, *Natural Hazards and Risk*, 9(1): 1280-1305.

Pradhan, B., U. Hagemann, M.S. Tehrany, and N. Prechtel, 2014. An easy to use ArcMap based texture analysis program for extraction of flooded areas from TerraSAR-X satellite image, *Computers & Geosciences*, 63: 34-43.

Raja, R.A., V. Anand, A.S. Kumar, S. Maithani, and V.A. Kumar, 2013. Wavelet based post classification change detection technique for urban growth monitoring, *Journal of the Indian Society of Remote Sensing*, 41(1): 35-43.

Ridd, M.K. and J. Liu, 1998. A comparison of four algorithms for change detection in an urban environment, *Remote Sensing of Environment*, 63(2): 95-100.

Rokni, K., A. Ahmad, A. Selamat, and S. Hazini, 2014. Water Feature Extraction and Change Detection

Using Multitemporal Landsat Imagery, *Remote Sensing*, 6(5): 4173-4189.

Salmon, B.P., W. Kleynhans, F. van Den Bergh, J.C. Olivier, T.L. Grobler, and K.J. Wessels, 2013. Land cover change detection using the internal covariance matrix of the extended Kalman filter over multiple spectral bands, *IEEE Journal of Selected Topics Applied Earth Observations Remote Sensing*, 6(3): 1079-1085.

South Asia Network on Dams, Rivers and People, 2017. State of India's River for India Rivers week, https://sandrp.in/2017/05/20/odisha-rivers-profile, Accessed on Feb. 5, 2016.

Sundaray, S.K., B.B. Nayak, S. Lin, and D. Bhatta, 2011. Geochemical speciation and risk assessment of heavy metals in the river estuarine sediments–a case study: Mahanadi basin, India, *Journal of Hazardous Materials*, 186(2-3): 1837-1846.

Tang, Z., W. Ou, Y. Dai, and Y. Xin, 2013. Extraction of water body based on Landsat TM5 imagery – A case study in the Yangtze river, *Proc. of 2012 International Conference on Computer and Computing Technologies in Agriculture*, Zhangjiajie, China, Oct. 19-21, vol. 393, pp. 416-420.

Upadhyay, S., 1988. Physico-chemical characteristics of the Mahanadi estuarine ecosystem, east coast of India, http://nopr.niscair.res.in/handle/123456789/38450.

Volpi, M., G.P. Petropoulos, and M. Kanevski, 2013. Flooding extent cartography with Landsat TM imagery and regularized Kernel Fisher's discriminant analysis, *Computers & Geosciences*, 57: 24-31.

Xu, Y.B., X.J. Lai, and C.G. Zhou, 2010. Water surface change detection and analysis of bottomland submersion-emersion of wetlands in Poyang Lake reserve using ENVISAT ASAR data, *China Environmental Science*, 30: 57-63.